# Modelling benthic invasion by the colonial gastropod *Crepidula fornicata* and its competition with the bivalve *Pecten maximus* . 2. Coupling the 0D model of colony-forming species to a connectivity matrix for a realistic distributed simulation of benthic invasion

Ménesguen Alain [1, *], Hachet Aloïs [1], Grégoris Thomas [1]

[1] Ifremer, Ctr Bretagne, Unite DYNECO, Lab LEBCO, CS 10070, F-29280 Plouzane, France.

* Corresponding author : Alain Ménesguen, email address : amenesg@ifremer.fr

**Abstract :**

The anthropogenic introduction in U.K. waters of the north-American marine gastropod *Crepidula fornicata* (Linné, 1758), commonly called slipper limpet, and its consecutive spreading has led in less than a century to the invasion of a part of benthic grounds along the North-European coasts. Competition for space has hampered the maintenance of the native scallop *Pecten maximus*, whereas dredge clogging has drastically limited scallop fishing, especially in the Western English Channel. In order to assess the possible future distribution and abundance of both species (*Crepidula* and *Pecten*), an original model of slipper limpet chains joined to a simple year-class model of the scallop (Ménesguen and Grégoris, 2017) has been coupled to a connectivity matrix summarizing the annual dispersion of emitted larvae in a realistic marine domain. This distributed model can explore the dynamics of both populations at the century scale and has been applied at two different geographical scales: a local one (the bays of Brest and Douarnenez, Western Brittany, France) and a regional one (Bay of Biscay and English Channel). First eigenvectors of the connectivity matrix are used to delineate the main retention areas. For each species taken alone, simulations starting with a few animals in different spots do converge in less than a century towards the same geographic distribution, compatible with the actual field distribution. This suggests that hydrodynamic patterns of larval drift create a strong attractor for these populations; it is reached by different routes of colonization, depending on the initial inoculation. The non-linear interaction created by the lack of space when the populations have filled the benthic area seems to be stronger for scallop populations than for slipper limpets, because of the permanent capacity of *Crepidula* beds to fix some larvae on the top of existing colonies. Whereas the scallop abundance experiences a rather large limit-cycle, with a dominant 11 years period and a lot of harmonics, the slipper limpet has commonly a stable steady state abundance. Competition between both populations tends to lower the mean scallop abundance and to lengthen and damp its fundamental period of oscillations. Simulated distributions can be locally improved by linking the larval survival to a distributed environmental stressor, as the salinity for scallop or a metallic contamination for the slipper limpet in the case of the bay of Brest.

**Highlights**

► A connectivity matrix describes the 40 days long larval drift of both species. ► Eigenvectors of this matrix delineate the main retention areas of larvae. ► Connectivity with matching matrix produces steady state maps of *Crepidula* colonies. ► Invasion by *Crepidula* halves the abundance of the harvested bivalve *Pecten* maximus.

# 1. Introduction

Since its first observation on oyster beds in Liverpool Bay in 1872, the marine gastropod *Crepidula fornicata* has invaded a lot of coastal benthic ecosystems along the coasts of the southern half of the UK, on the French side of the English Channel, along Belgium and the Netherlands. Its northward progression seems to be stopped by the too cold temperatures (Thieltges et al., 2004). Several papers have reported new sites of colonization, and some have attempted a global compilation of the sites where the species has been observed in the North-East Atlantic (Blanchard, 1997, Fig. 1). The most extended populations present along the French coasts have been observed first in the Golfe Normand-Breton (Quiniou and Blanchard, 1987), especially the bay of Saint-Brieuc (Hamon and Blanchard, 1994), and secondly, in the bay of Seine (Leblanc et al., 2011). The abundances observed in the bay of Saint-Brieuc (Blanchard et al., 2001) are around 3000 ind.m$^{-2}$ in dense beds (coverage > 70%), and around 1000 ind.m$^{-2}$ in more sparse populations (40% < coverage < 70%); but Blanchard (2005) found up to 4 000 ind.m$^{-2}$ in the bay of Mont Saint-Michel and Quiniou and Blanchard (1987) 9000 ind.m$^{-2}$ around the Chausey Islands, in the Golfe Normand-Breton. On the Atlantic coast, the main spots are smaller, in the bay of Brest (Guérin, 2004) and the Marennes-Oléron bay (Sauriau et al., 1998). A recent compilation of recorded presences of slipper limpets in historical samples taken in the southern part of the English Channel (Blanchard, 2012) (Fig. 2 upper panel) and the corresponding compilation for the northern part of the English Channel by the National Biodiversity Network's Gateway (Fig. 2, lower panel) ascertain qualitatively the presence of the slipper limpet on the French side of the English Channel, from the bay of Saint-Brieuc up to the Belgian frontier (and its absence in the north-western part of Brittany), as well as its presence in the shallow strip around UK. The apparent lack along the Picardy coast (French side of the Eastern English Channel) mentioned in 1997 has been filled in the 2011 map and confirmed in 2013 by Augris and Clabaux (2013), who recorded dense *Crepidula* beds near the coast of Fécamp and Saint-Valéry en Caux. In the bay of Brest, the distribution observed in the field till the end of the 20$^{\text{th}}$ century (Fig. 3, top panel, from Coum, 1979) has regressed during the last decade (Fig. 3, bottom panel, from Carlier, pers. comm.). Assessing from field data the effect of the slipper limpet invasion on the scallop distribution is not easy, because distribution maps of the scallop populations are recent and show more the modified distribution than the pristine one, as well for our local site where scallops are confined in the middle of the bay of Brest (Fig. 4, top panel from Thouzeau et al., 2000) as for our regional site, where distribution of active fishing areas appears to be peripheral (Fig. 4, bottom map, from Le Goff et al., 2017).

Two questions then arise: 1/ has the species reached nowadays its maximum extent (if not, which areas will it invade furthermore?), 2/ can we expect a future regression of the colonized area?

Even if anthropogenic actions (maritime transport, discharge to the sea of dredging wastes…) have had a decisive seminal role, the answer to the first question is now strongly linked to the natural dissemination potential of the larval stage of this species. The hydrodynamical modelling of the coastal seas under concern can then bring a reliable support to this question, by giving the geographic distribution of tracers released from any marine position and transported during the larval phase duration.

The second question depends on many poorly known processes (interspecific competition, infections by viruses and bacteria, toxic effects of chemical pollutants or phytoplanktonic toxins…), so the long term observation is necessary to get plausible answers.

Models which have explored the dissemination/settlement of benthic populations are mainly based on lagrangian simulation of larvae, i.e. they simulate the trajectories of numerous larvae (or batches of larvae) released from single or multiple locations at different dates (Cowen et al., 2000; Ayata et al., 2010; Andutta et al., 2012). A statistical analysis of the trajectories can show the trapping areas, created by local, bathymetry-driven modifications of the flow field, the so-called "sticky water effect" (Wolanski, 1994). Some models however deal with larvae as eulerian variables (Alexander and Roughgarden, 1996; Bendtsen and Hansen, 2013). Whatever the type of model used (eulerian or lagrangian), the exchanges of larvae between different places in the domain can be computed and gathered in a connectivity matrix. In the growing literature on connectivity, several approaches can be found to analyse the topology of the dispersal network. Whereas Treml et al. (2008) relied on graph theory, Nilsson Jacobi and Jonsson (2011) used the eigenvalues of the connectivity matrix (and especially the value of the leading one) to assess the persistence of subpopulations thanks to the perturbation method. As the eigenvectors themselves don't seem to have been used until now, we propose in this study their use to map the main retention regions, if the connectivity matrix ensures a complete cover of the discretized area under study. The synthetic 2D model of larval dispersion brought by the connectivity matrix is easily coupled to a previously described 0D model of the chain-forming slipper limpet (Ménesguen and Grégoris, 2017) to simulate the many decades long invasion phase, and to map the climax steady state distribution of this gastropod species. A similar model of the scallop, a non-colonial bivalve, is then run in competition with the slipper limpet one. The unique case of observed strong regression of a dense slipper limpet population (in the southern part of the bay of Brest) is used to test a putative harmful effect of heavy metal pollution on the *Crepidula* larvae.

## 2. Material and methods

### 2.1. The connectivity matrix

In order to simulate the larval drift occurring during the pelagic larval phase (i.e. a maximal 40 days duration), as well for the gastropod *Crepidula fornicata* as for the bivalve *Pecten maximus*, a 3D hydrodynamical model of the region of interest has been run from May, 20 to June, 30 of the year 2000. The MARS3D hydrodynamical code (Lazure and Dumas, 2008) has been applied first to the French Atlantic shelf, using a regular grid with 4 x 4 km meshes and 30 sigma levels and covering the Bay of Biscay, the English Channel and the southern part of the North Sea, up to the Rhine estuary (Fig. 5, left panel). For a more local extent, the same code has been applied to the two bays of Brest and Douarnenez, at the western end of France, using a regular grid with 0.75 x 0.75 km meshes and 10 sigma levels (Fig 5, right panel). The connectivity between an emitting mesh and a receiving one of the model grid is defined here as the fraction of a conservative tracer initially placed only in the bottom layer of the emitting mesh which is retrieved 40 days after in the receiving one. The tracer may be a dissolved one, or a particulate one having a settling velocity. The tracer fraction in the receiving meshes may be computed diversely: we can sum up the total tracer present in the receiving water column, or keep only the fraction present in a specific layer, for instance the bottom one. If the model grid contains *m* water meshes, a *(m+1). (m+1)* matrix of connectivity *M* will be constructed and then used every year to compute the annual transport of larvae over the domain. For our regional case, *m*=3513, whereas *m*=814 in our local case. The first row gives the tracer quantity entering the domain during the simulation duration (i.e. zero in the general case), and the first column gives the tracer quantity which has left the domain at the end of the simulation. Owing to the rapid increase of memory necessary to store during a century the age-class structures of the distributed population model, meshes of the hydrodynamical basic grid have been pooled into square "super-meshes" of 3 x 3 meshes for the regional model, and 2 x 2 meshes for the local model. If the "super-mesh" contains only water basic meshes, its initial tracer concentration will be set to 1.0, whereas if it contains *w* water meshes and *t* terrestrial meshes, the initial tracer concentration will be set to *w/(w+t)* only. The coarse grid on which the connectivity matrix has been computed will be referenced as the "super-grid" thereafter.

This connectivity matrix summarizes the effect of the various circulation patterns which have been active in the region of interest during this 40 day period of dispersion; these patterns can be disentangled by diagonalization of the matrix. All the eigenvalues of the connectivity matrix have a module strictly lower than 1.0, some of them are real, the other are pairs of conjugate complexes. If a tracer is initially distributed following

the eigenvector $U^{(0)}$, associated to the strictly positive eigenvalue $\lambda$, its distribution after $n$ years of dispersion will be given by $U^{(n)} = M^n \cdot U^{(0)} = \|\lambda^n\| \cdot U^{(0)}$. As $\|\lambda\| < 1$, the tracer concentration gradually vanishes. So, if we rank the eigenvalues in descending order of modules, the first eigenvectors will give the more remanent patterns, and hence reveal the areas which are the most capable of retaining pelagic larvae and hosting dense benthic populations.

## 2.2. The biological population models

The 0D models of the slipper limpet colonies and the scallop population (with or without interaction), described in the first part of this paper (Ménesguen and Grégoris, 2017), have been replicated in each mesh of the "super-grid". In order to take into account a space requirement different for each species, a bottom "vital area" is assigned to each animal: for the slipper limpets, which can live side by side on the ground, it is equal to their real ventral surface, whereas it is 50 times bigger for scallops, which always maintain a distance between themselves. A distributed initialization must be specified for each of these species. To study the capability of colonization/invasion, and the paths taken, only one "super-mesh" has been inoculated, but with a rather dense population of benthic adults, in order to have a good chance of dissemination (200 individuals.m$^{-2}$ of every age class for the slipper limpet, and 5 individuals.m$^{-2}$ of every age class for the scallop). The spreading of initial population is then entirely driven by the release of pelagic larvae and their dispersion according to the connectivity matrix. As pointed out in the previous 0D model presentation, the final success of the colonization is very sensitive to the larval survival rate. Downscaling the "super-mesh" size, for instance here from 12 x 12 km at regional scale to 1.5 x 1.5 km at local scale, increases the connectivity values by a factor 100, i.e. decreases the mean loss from mesh to mesh caused by the dilution, as well as the probability of being eaten by predators. In order to maintain the same global probability of recruitment, a re-calibration of the annual survival rate of larvae is required as soon as we change the mesh size or the thickness of the bottom water layer from which the larvae can settle on the sea floor. When the larvae, able to settle, are taken only in a 1 meter thick bottom layer, the calibrated survival rates have been finally set to 0.015 y$^{-1}$ at the regional scale and 0.1 y$^{-1}$ at the local scale for slipper limpet, and 10$^{-6}$ y$^{-1}$ both at local and regional scales for scallop. The slipper limpet larvae are strongly attracted by existing benthic adults, but can however settle on bare grounds, with a probability fixed at $\alpha$=0.01 at regional and local scales.

The competition for space between the two species is not symmetrical, because slipper limpets can settle upon scallop shells, but not vice versa. Moreover, the scallop is able to swim near the bottom, whereas the creeping capacity of the slipper limpet vanishes for adults and make them almost sedentary. The model allows

slipper limpet chains to form on scallop shells, and limits the settlement of scallops on *Crepidula* beds by considering that a bottom already partially occupied by slipper limpets has a fitness β ($0 \leq β \leq 1$) for scallop. From the scallop's "point of view", the current bottom coverage is then the scallop coverage, increased by (1- β) times the slipper limpet coverage. As the 0D model (Ménesguen and Grégoris, 2017) has shown that the speed of initial growth of a bivalve can modulate the period of its limit cycle, we have taken two different values for the K parameter of the scallop von Bertalanffy growth curve. For the whole regional model, which covers wide oligotrophic areas, we have used the low value (K = 0.545) observed in the bay of Saint-Brieuc (Antoine, 1979), whereas for our local model, which covers a more eutrophic area, we have taken the rather high value (K = 0.83) observed in the bay of Brest (Chauvaud et al., 2012).

### 2.3. The distributed stressors

In order to improve the realism of the final distribution, the possibility of a deleterious effect on drifting larvae has been introduced. The common survival rate of larvae from spawning to benthic recruitment has been multiplied in each "super-mesh" by a fitness factor of the local sea water, varying between 0.0 (water totally unsuitable for the larval life) to 1.0 (water totally favorable to the larval life). This fitness factor depends on the corresponding stressor through a classical sigmoid dose-response relationship.

For the scallop, the main and ubiquitous stressor considered in this study is the salinity, because scallop larvae and spat are known not to survive in brackish waters of salinity < 25 (Christophersen and Strand, 2003). The annual 10th percentile of the surface salinity computed by the MARS3D hydrodynamical model (used to compute the connectivity) has been mapped on the "super-grid" and used as driving variable S in the logistic equation (1), in which $f_1$ and $f_2$ are calibration parameters:

$$f(S) = \frac{1}{1+f_1.e^{-f_2.S}} \qquad\qquad (Eq.1)$$

Figure 6 gives the graph of the function f(S) used, and the resulting maps of salinity stress at regional and local scales.

For the slipper limpet, the mass mortality of *Crepidula* beds observed in the southern part of the bay of Brest during the last decade (A. Carlier, pers. comm.) has drawn the attention on the possible toxic effect of heavy metals brought by the Aulne River, which originate from an ancient silver lead mine. Slipper limpet fecundity (Nelson et al., 1983) as well as larva survival (Nelson, 1978) are known to be particularly sensitive to silver contamination. The French national pollutant monitoring network (ROCCH) has recorded in 2000 a sudden rise (for unknown reasons) in oyster silver contamination at the mouth of Aulne River (see ROCCH

stations on Fig. 7), and this high level of contamination has been recorded up to now. As an increase of dissolved silver brought by the Aulne water could promote some deleterious effect on slipper limpet larvae, the decadal median dilution plume of the Aulne river has been computed by Ménesguen and Dussauze (2015) over the 2000-2010 decade thanks to the same MARS3D model used here, and taken as a normalized proxy of the dissolved pollutant concentration P. P is used as driving variable in Eq. 2, derived from a logistic formulation ($g_1$ and $g_2$ are calibration parameters):

$$g(P) = 1 - \frac{1}{1+g_1.e^{-g_2.P}} \qquad \text{(Eq. 2)}$$

The left panel of Fig. 7 gives the graph of the function g(P) used, and the central panel shows the resulting map of toxic stress at the local scale of the bay of Brest. The right panel of Fig. 7 gives the time series of silver concentrations measured in oysters at two ROCCH stations located at the mouth of Aulne River and Elorn River respectively.

Finally, if we summarize into the function s the spawning effort of the local population and into the function b all the annual transformations of the local demography detailed in the 0D model, the global 2D model may be summarized by Eq. 3 and 4:

*Vector of settling larvae in m meshes during year t*: $\vec{L^t} = M.S.\overrightarrow{s(N^t)}$  (Eq.3)

*Vector of p age classes in m meshes at year t + 1*: $\overrightarrow{N^{t+1}} = \overrightarrow{b(N^t, L^t)}$  (Eq.4)

$\vec{N^t}$  vector (m x p components) of p age class abundances in m marine meshes of the grid BEFORE annual biological evolution

$\overrightarrow{b(N^t, L^t)}$ vector (m x p components) of p age class abundances in m marine meshes of the grid AFTER annual biological evolution

$M$  connectivity matrix

$S$  diagonal stressor matrix, giving the local survival probability of larvae spawn in each marine mesh.

Table 1 summarizes the values of the various parameters used in the 2D model for both species. As detailed in the following section, this distributed model has been used first for each species alone, to compare the different transient phases corresponding to various places of first inoculum, and to map the steady state of the

final distribution, and the limit cycle if any. Then, using both species distributed models together will show the effect of competition between scallop and slipper limpet.

## 3. Results

### 3.1. Preferential pathways of colonization and steady state distribution of the two species alone

As a result of a trial of various connectivity matrices obtained for dissolved or particulate tracers, which were computed whether for the only one meter surface layer, or for the one meter bottom layer, or for the whole water column, the more realistic results at both regional and local scales have been found for dissolved tracers in one meter layers, near the bottom for the slipper limpet and near the surface for the scallop. The eigenvalues of the bottom connectivity matrices ranked in descending order of module (Fig. 8) show higher first values (hence more persistent patterns), but a quicker decrease (hence less complex global figures) in the local case than in the regional one, because confining pathways may be expected to be more numerous but more dispersive in a large and heterogeneous region (as the bay of Biscay-English Channel system) than in a small system (as the bays of Brest and Douarnenez). The first two eigenvectors (Fig. 9) isolate estuaries: Bristol Channel and Thames at the regional scale, Aulne and Elorn Rivers at local scale. The following eigenvectors (Fig. 9) isolate confining areas. At the regional scale, these are the Belgian coastal strip, the bay of Seine and the Golfe Normand-Breton, the southern margin of the continental shelf off Brittany, the entrance of the English Channel including the Iroise Sea. At the local scale, they are associated to the central part of the bay of Brest and to the bay of Douarnenez respectively. Simulated colonizations, which have been performed using the parameter values given by Table 1 and a mean annual, time-invariant salinity field to assess the survival probability of scallop larvae, show that whatever the distribution of the inoculum, the population accumulates in the regions delineated by these first eigenvectors of the connectivity matrix, beginning by those which are the closest to the inoculum point, and reaching eventually the farthest ones if the larval survival rate is high enough. This reflects the fact that in the first years of spreading, the colonization is mainly driven by the linear process of larval transport, and is mainly featured by the properties of the connectivity matrix. Non-linear density dependence processes will only become important when the bottom coverage has reached a high percentage.

In our local example, whatever the location of the inoculum of slipper limpets, the settlement begins mainly in the eastern part of the bay of Brest (Fig. 10), i.e. the Elorn estuary and the bay of Daoulas and Aulne estuary pointed out by the two first eigenvectors, which is in accordance with the distribution observed in the field up to the end of the 20th century (Fig. 3, top panel) by Coum (1979). Then the colonization invades partially the central and western part of the bay, in agreement with the third eigenvector. If the larval survival rate of the slipper

limpet does not exceed 0.23 y$^{-1}$, the bay of Douarnenez (located south of the bay of Brest) does not allow successful settlement of benthic colonies and remains free of *Crepidula* beds. The duration of this expansion phase is very dependent on the probability α of settling on bare grounds. With α = 0.01, it takes about 40 years to reach a steady state distribution from scratch, but a 23% more crowded steady state is reached in only 20 years if α = 0.05. The final steady state is a stable distribution (Fig. 11, top panel). Simulated and observed abundances are in the same order (around 1000 ind.m$^{-2}$ observed in the Elorn estuary, around 300 ind.m$^{-2}$ in the middle of the southern part of the bay of Brest), but the model cannot reach the maximum density of 3500 ind.m$^{-2}$ observed in one station. The distribution observed since 2000 (Fig. 3, bottom panel) needs the introduction of a specific stressor. Using the 90$^{th}$ percentile of the Aulne water dilution in the surface layer of the bay of Brest as a proxy of a contamination caused by the Aulne River brings a real improvement (Fig. 11, bottom panel), causing the decline of slipper limpets populations in the southern part of the bay of Brest, and their total extinction from the embayments close to the Aulne mouth. The fact that measurements in oysters *Crassostrea gigas* taken at Aulne ROCCH station (Fig.3, right panel) have shown a sudden increase of silver content around 2000 and have kept a high contamination up to now is in favor of a recent modification of contamination, for an unknown reason, but experimental demonstration of Aulne water toxicity on *Crepidula* larvae is still lacking.

In our regional example (Fig. 12), the invasion of the slipper limpet will not systematically reach rapidly the same global steady state, because at this scale, the general tidal residual circulation can delineate some quasi-independent sub-regions that will confine the drifting larvae. Colonization will then be rapid only in the confining areas downstream (in the sense of the tidal residual drift) from the inoculum point, even if it can also reach more slowly some upstream areas, thanks to turbulent dispersion caused by the alternating tidal currents. The continental shelf region under concern can be divided at least into 4 sub-regions of settlement: the south of Irish Sea, the U.K side of the English Channel, the French side of the Eastern English Channel (from the Golfe Normand-Breton up to the Belgian zone), and the French coastal strip of the bay of Biscay. The duration of the expansion in these sub-regions depends on the connectivity levels inside them and the number of successfully recruiting larvae per benthic adult. In the case of the slipper limpet, when the larval survival rate does not exceed 0.02 y$^{-1}$, only inoculation meshes not far from confining regions can produce a wide successful settlement. Whereas inocula put along the U.K. coast of the English Channel do not succeed in creating significant settlement, an inoculum put into the bay of Seine (East English Channel) turns into a population which invades the coastal strip up to the Belgian coast in less than 100 years (Fig. 12, upper panel), then goes westwards on both sides of the English Channel, i.e. around the Cotentin peninsula into the Golfe Normand-

Breton on the French side, and along the English south coast up to Cornwall (which is reached after 350 years)on the U.K side; invasion of the Bristol Channel and the southern Irish Sea requires 500 years. Because of its higher probability of recruitment and its quicker bottom coverage, the scallop illustrates better than the slipper limpet the various pathways and timings of colonization obtained with different inoculated zones. If the inoculum is located in the Atlantic bay of Marennes-Oléron (in the middle of the French coast of the bay of Biscay), the population is restricted during the first century to embayments along the French Atlantic coast (Fig. 12, middle panel), but after turning around the Brittany peninsula, it can rapidly occupy the Golfe Normand-Breton, from which it suddenly invades in a decade the whole English Channel and southern Bight of the North Sea, to finally reach the southern Irish Sea after 120 years. Inversely, an inoculum located in the vicinity of the Isles of Scilly (northern entrance of the English Channel) gives a main clockwise pathway, almost opposite to the former (Fig. 12, bottom panel), but travelling more quickly (70 years instead of 120 years). Of particular interest in this case is the weak secondary counterclockwise pathway, which crosses southwards the entrance of the English Channel and the Iroise Sea, in accordance with the $6^{th}$ eigenvector mapped in Figure 9; this might ensure the possible colonization of the Bay of Biscay continental shelf by populations proceeding southwards from the Devon and Cornwall coasts.

For the slipper limpet, as far as the larval survival rate is not above 0.02 $y^{-1}$, the simulated steady state distribution obtained from several simultaneous inocula shows in the regional case (Fig. 13) a quasi-total coverage of the bottom in the favorable areas, without any significant oscillation. The whole Bristol Channel, the English Channel and the Southern Bight of the North Sea are invaded, more densely near the coasts, with a highest abundance in the areas pointed out by the first eigenvectors of the connectivity matrix, i.e. the Golfe Normand-Breton, the bay of Seine and the coastal strip joining it to the Belgian waters. This simulated distribution of the slipper limpet is qualitatively compatible with the observed colonization of NW European coasts schematized (Fig. 1) by Blanchard (1997). The model reproduces the most extended populations present along the French coasts of the English Channel (Golfe Normand-Breton, bay of Seine), as well as the absence of slipper limpets in the north-western part of Brittany. The simulated presence in the shallow strip around UK is compatible with the qualitative data available (see Fig. 2) and the two existing small spots along the Atlantic coast (bay of Brest, Marennes-Oléron bay) are well retrieved by the model. As far as the transient dynamics of colonization is concerned, the simulated westward expansion (i.e. in the opposite way to the residual current circulation) along the southern U.K coast when the inoculum is put in the eastern English Channel is corroborated by the observation, made during the first half of the $20^{th}$ century, that the slipper limpet was first

established in the Solent and has spread westward, to Weymouth and West bay (Holme, 1961). In the simulated steady state as well as in the real world, the south-western coast of Ireland appears to be still free from slipper limpets, even if some small individuals have been recorded in 1993 near Dungarvan Bay (Mc Neill et al., 2010), which is in accordance with the low abundances simulated in this area by the model (Fig. 13). But the scarce observed presences in areas deeper than 20m in the Golfe Normand-Breton and in the Eastern Channel suggest that the real abundance of slipper limpets in these regions is presently considerably lower than the medium values produced by the model. On the contrary, in densely crowded sites, the model underestimates densities (about 1600 ind.m$^{-2}$ only in spite of a simulated 95% coverage), probably because the hypothesis of a pure one-layer occupation of the ground (i.e. the sum of ventral areas of animals situated at the base of the colonies not exceeding the total ground area) prevents the model from simulating extremely high densities, namely $\geq$ 3000 ind.m$^{-2}$. The mean distribution of chain lengths simulated in the Golfe Normand-Breton reproduces correctly the distributions observed in 2002 at the stations 197 and 210 (for location, see part 1 of this paper, Ménesguen and Grégoris, 2017), with a modal length about 4 animals for primary chains and an exponential-like distribution for the secondary chains (Fig. 14). But, in these two stations not completely invaded, as in several other areas presently not densely colonized by slipper limpets, the model overestimates the number of chains and, hence, locks on a modal length of 4 rather than 3 animals.

For the scallop, as far as the larval survival rate is not lower than one larva per million, the population succeeds in invading almost the whole continental shelf, proceeding from the well-connected sub-region containing the inoculation point to the next. The final simulated steady state distribution of scallop exhibits higher abundances in the peripheral shallow waters. Whereas scarce populations do reach a constant steady state abundance, dense populations reach a periodic final state, a so-called limit cycle. For instance, the steady state population obtained in the bay of Brest oscillates with a 11 year period from a "northern" to a "southern" distribution (Fig.15, upper panel), in a stationary wave mode (seiche). At the regional scale, the dense populations of the English Channel show also a pronounced oscillation having a main period around 11 years and travelling from the coast towards the deeper waters (Fig. 15, lower panel). The colonization of the bay of Biscay continental shelf is restricted to a coastal shallow strip.

The simulated distribution of scallop alone in the bay of Brest (Fig. 16, upper map) reproduces the ubiquitous distribution observed by Faure (1956) before the strong colonization of the seabed by the slipper limpet, and the simulation with spatial competition exhibits a scallop population restricted to the center of the bay, in agreement with the actual distribution (Fig. 4, top panel), as described by Thouzeau et al. (2000). These

authors have pointed the invasion by the slipper limpet of some parts of the bay of Brest as being the most plausible cause for the decrease of scallop populations in these areas. In the English Channel, the simulated scallop distribution mimics the peripheral distribution of active fishing areas schematized in Fig. 4 (bottom panel). Although calculated on a large grid mesh (12x12km) and with an annual time step, our steady state distribution in the English Channel retrieves the features of the map produced by the 30 year simulation by Le Goff et al. (2017), who have used, 30 days per year, the MARS3D model on a fine grid (2x2 km) and with a time step ≈ 5 mn to simulate the larval drift. The simulation shows also some scallops along the French coast of the bay of Biscay (where some catches and landings do attest their presence). The simulated colonization at the western end of Brittany mirrors weakly the observed population barring the English Channel entrance. Existence of this fishing area supports the behavior of the model, which links the western Cornwall region to the Iroise Sea, in front of western Brittany, in accordance with the 6th eigenmode type showing a vast trapping zone in the Western approaches of the English Channel (Fig. 9). Even if it underestimates its abundance, the model suggests that the well-known and exploited scallop population located on the Armen sand-bank, western from the Sein island (see the red point named Armen on Fig.4), could be more linked to the western English populations than to the ones located on the French side of the English Channel.

### 3.2. Competition between the slipper limpet and the scallop

Four fitness coefficients β (0.4, 0.5, 0.6, 0.8) have been tested at the local scale, where a recent precise distribution map of scallop abundance is available (Thouzeau et al., 2000). When β decreases, the scallop density drops strongly in shallow areas in front of estuaries, where the slipper limpet beds are the densest. The best matching with the recent distribution of scallops (Fig. 4, lower panel) is obtained for β around 0.5. The comparison with the "no competition" simulation (β = 1.0) suggests that the actual abundance of scallop in the bay of Brest has been severely lowered by slipper limpet competition in the anciently very favourable eastern embayments, and mainly restricted to the center part of the bay (Fig. 16). At the regional scale, for β = 0.5, the scallop population shows also a substantial reduction of abundances relatively to the "no competition" situation, especially in the favourable bays along the French coast of the English Channel (Golfe Normand-Breton and bay of Seine), where the loss may amount 50%, but remains unchanged west from the entrance of the English Channel and along the French Atlantic coast (Fig. 17). Globally, the total abundance of the scallop over the whole regional domain decreases by 30% when β drops from 1.0 to 0.5 and by 18% over the local domain.

## 4. Discussion

With respect to the geographic distribution of species, this study shows that oceanic connectivity matrices can unravel hidden spatial structures through their first eigenmodes, as do brain connectivity studies (Becker et al., 2017). Connectivity matrices derived from field data (e.g. tagging experiments on swimming species) generally do not map continuously the area under study, but gives only the links between dispersed spots. The lagrangian approach used in Individual-Based-Models (IBM) also produces usually non-continuous spatial connectivity matrices, so the methods used to extract retention areas from these discrete connectivity matrices come from network analysis and cluster analysis. Recent examples of such approach have been performed on coral reefs in Indian Ocean (Crochelet et al., 2016; Mayorga-Adame et al., 2017). In our study aiming at long term simulations without insight in individual larval history and path, we have chosen the eulerian approach, owing to its straightforward coding in hydrodynamical 3D models and to the conclusion of Nicolle et al. (2015), who found no significant differences between the lagrangian and eulerian modelling of larval drift in the English Channel. In our perspective, the advantage given by eulerian modelling of tracers is to naturally build a connectivity matrix covering the whole space continuum of the area under study, so that its eigenvectors can be visualized as maps. Ranking these eigenmodes by decreasing order of the associated eigenvalues shows immediately where the main retention areas are. As no previous ecological study seems to have used this eigenmode approach of connectivity matrix, several questions however remain unclear. In pure linear algebra, any recurrent use of the same connectivity matrix would always produce successive geographic distributions converging towards the first eigenvector, associated with the eigenvalue having the highest module (i.e. the closest to 1). In benthic population models as ours, saturation of the substratum introduces progressively a strong non-linearity in the model, and moves the model behavior far from the simple pure linear one. The possible shift to less dominant eigenmodes of the connectivity matrix remains unclear.

The mechanisms taken into account during the computation of the connectivity matrix can be numerous and several recent studies have added to pure physical processes more and more biology-driven ones. Drake et al. (2013) show for instance that in case of strong offshore drift in the surface layer during an upwelling event, invertebrate larvae released from central California can however be retained within 5 km of the coast at 30 days if they move under the surface layer. Similarly, Paris et al. (2007) showed that computed settlement success was enhanced in different regions of the Caribbean Sea when a shallow ontogenetic vertical migration behavior was assigned to the simulated larvae. For *Crepidula fornicata*, observations indicate that larvae sink in calm water and swim up in stronger turbulence, and show some downward movement during ebb and low tides and

upward movement during flood and high tides (Fuchs et al., 2010). For *Pecten maximus* in the English Channel, Nicolle et al. (2015) tested the modifications induced in connectivity when using a temperature-dependent larval duration and a complex swimming behavior based on observations, i.e. starting with a neutrally buoyancy of eggs and small larvae, changing to increasing, then decreasing, upward swimming and ending the pelagic life with a quick sinking after the retraction of the velum. Focusing on two large embayments in the English Channel (bays of Seine and Saint-Brieuc), these authors concluded that temperature-dependent planktonic larval duration can really improve the realism of simulated dispersal, whereas swimming behavior has a minor effect on it. For the sake of simplicity, and because we iterate the annual connectivity matrix over many decades and large areas to compute long term, large extent steady state distributions rather than transient ones, high spatial resolution maps, we have kept the simplest and most ancient approach with no specific biological behavior, i.e. to consider only the advection-diffusion processes governing the distribution of pure dissolved conservative tracers, and apply a global mortality rate to the pelagic larval stage.

The question of competition for space is not a new one in ecological modelling. The competition between members of a single species population has been taken into account by introducing an asymptotic maximum abundance in the Malthusian exponential model, which led to the logistic growth curve of a single population (Levins, 1969). For two or more interacting species, Tilman (1994) proposed an asymmetric version of the Lotka-Volterra equations, where a dominant or 'superior' species coexists with a dominated or 'inferior' one. For the 'superior' species, the constraint on maximum abundance depends of its own abundance only, whereas it depends on the two species total abundance for the 'inferior' one; the Lotka-Volterra classical interaction term is kept only for the 'inferior' species. The population interaction model presented in our study can be viewed as an age-structured expansion of this theoretical model of total abundances: the slipper limpet would be the 'superior' species, and the scallop the 'inferior' one, even if Tilman considered the 'inferior' species as the invader, a situation inverse to ours. The Tilman's model explains why the dominated species may however subsist among the dominant population and can be generalized to several species. The transient regime from initial state to final steady state may or not exhibit damped oscillations. More recently, Crowley et al. (2005) kept the symmetry of seminal Lotka-Volterra equations in the growth limitation term and re-formulated the initial interaction term in a so-called "overgrowth" term. These general equations show that the system can evolve either towards a monospecific population (the eliminated species depends on the initial abundances and the parameter values) or towards a stable equilibrium between the species. All these non-linear models however don't produce stable oscillations (limit cycles) as ours do for the scallop. The possible theoretical occurrence of

limit cycles in populations fixed on a substratum seems to have been noticed first by Roughgarden et al. (1985), thanks to a model in which competition for space between adults changes with time, according to the place occupied by growing animals. They observed that "interference of growth with recruitment can prevent the steady state from being stable, and can cause, as one of the possibilities, a limit cycle oscillation". Roughgarden et al. (1985) applied their model to barnacles, and a similar approach was used for an octocoral overgrown by a colonial ascidian when it is young, but not when it has reached a greater size (Sebens, 1982). Although it deals with unattached species living on soft bottoms, our model exhibits the same limit cycle behavior as these previous models of species attached on hard bottoms. Our model, which links the spatial competition to the size distribution of the animals, and not to their total abundance, exhibits a 11 year limit cycle in the dense scallop populations in the English Channel; this calls to mind the periodic oscillations observed in the scallop catches in the English Channel, but also in various populations of Pectinidae (see discussion of the 0D model, Ménesguen and Grégoris, 2017). Interestingly, such stable oscillations don't appear in the previous distributed population models developed on the whole English Channel, either for the banded carpet shell *Paphia rhomboides* (Savina and Ménesguen, 2008) or the scallop (Le Goff et al., 2017). For instance, starting with a uniform adult distribution, Le Goff et al. (2017) obtain after 20 years a mean steady state scallop distribution very similar to ours, but without any limit cycle. This is due to the fact that their model treats the competition between adults as a global density-dependent additional mortality, uniform for all age classes. This black box parameterization, which mixes competitions for food and for space and does not link competition for space to the size of the animals, proves to be unable to generate a periodic behavior. Then, introducing an explicit formulation of competition for space in the benthic populations models does help to capture complex non-linear interactions within and between species.

**5.    Conclusion**

Using a connectivity matrix to summarize the 5 weeks drift of pelagic larvae of the gastropod *Crepidula fornicata* and the bivalve *Pecten maximus* has allowed to explore quickly the long term evolution (i.e. over a few centuries) of these two benthic invertebrates, either alone or in competition for benthic space. Through its first eigenvectors, the connectivity matrix reveals the main confining sub-regions of the domain, which can be used as proxies for the main settlement areas of the species. At the local scale (embayments) as well as at the regional one (bay of Biscay or English Channel), these areas are primarily located in shallow zones bordering the land, in front of some estuaries (Severn, Thames, Seine, Elorn, Aulne, Charente…) and in some embayments (Golfe Normand-Breton, bay of Marennes-Oléron…). The simulations confirm that whatever the initial inoculation made on the continental shelf, both species reach a steady state distribution, compatible with their observed distributions. *Crepidula fornicata* reaches its stable steady state more slowly than *Pecten maximus*, which exhibits a clear limit cycle having a period about 11 years in the areas where the environment is favorable to the species. The length distribution of the stacks built by the slipper limpet locks on a unimodal distribution (mode = 4 ind./chain) for the primary chains, and on an exponential-like distribution for the secondary chains attached to the primary ones. This ordered stacking is a feature which seems specific to slipper limpet populations, but our approach could probably be adapted for epibiontic species (barnacles, bryozoans…). Our model, based on the hypothesis that competition between *Crepidula fornicata* and *Pecten maximus* is deleterious for *Pecten* only, shows a decrease of the scallop population mean abundance (with a damping of its natural oscillation) and mimics the observed fouling of scallop shells by slipper limpet colonies of various lengths. The model indicates that the native scallop populations lost around 50% of their initial densities in the regions strongly invaded by the invasive species *Crepidula fornicata*. The steady state distribution computed for the slipper limpet seems to be wider than the actual observed one, especially towards the deeper parts of the shelf. This suggests that the diverse food carrying capacities of the continental shelf areas should now be taken into account to modulate the fecundity and then, to state more confidently if the spreading of *Crepidula fornicata* is still in progress.

**Acknowledgements**

**References**

Alexander, S. E., Roughgarden J., 1996. Larval transport and population dynamics of intertidal barnacles: a coupled benthic/oceanic model. Ecological Monographs , 66, 259–275.

Andutta F., Kingsford M., Wolanski E., 2012. 'Sticky water' enables the retention of larvae in a reef mosaic. Estuar. Coast. Shelf Sci., 101, 54-63.

Antoine L., 1979. La croissance de la coquille Saint-Jacques *Pecten maximus* et ses variations en Mer Celtique et en Manche. PhD thesis,  Université de Bretagne occidentale, 148 p.

Augris C., Clabaux P., 2013. Cartographie morpho-sédimentaire des petits fonds marins ; du cap d'Antifer au cap d'Ailly. Atlas, éditions QUAE, 80 p.

Ayata S.-D., Lazure P., Thiébaut É., 2010. How does the connectivity between populations mediate range limits of marine invertebrates? A case study of larval dispersal between the Bay of Biscay and the English Channel (North-East Atlantic). Prog. Oceanogr., 87, 18-36.

Becker C. O., Pequito S., Pappas G. J., Miller M B., Grafton S. T., Bassett D. S., Preciado V. M., 2018. Spectral mapping of brain functional connectivity from diffusion imaging. Scientific Reports, 8:1411.

Bendtsen J, Hansen JL, 2013. A model of life cycle, connectivity and population stability of benthic macro-invertebrates in the North Sea/Baltic Sea transition zone. Ecol. Model., 267, 54– 65.

Blanchard, M., 1997. Spread of the slipper limpet (*Crepidula fornicata*) in Europe. Current state and consequences. Scientia Marina, 61, 109-118.

Blanchard M., 2005 – Dynamique de la population de crépidule (*Crepidula fornicata*) en baie du Mont Saint-Michel. Rapport Ifremer DYNECO/EB/05.01: 33p. http://archimer.ifremer.fr/doc/2006/rapport-5901.pdf

Blanchard M., 2012. La crépidule et la coquille Saint-Jacques en Manche ; inventaire et impacts. Rapport Ifremer/Dyneco-EB/12.02/mb, 39 pages + annexes.

Blanchard M., Blanchet A., Gaffet J.-D., Hamon D., 2001.Dynamique de population de la crépidule (*Crepidula fornicata*) en baie de Saint-Brieuc (Manche-Ouest). Rapport Ifremer RST.DEL/00.08/Brest, 60 p. + annexes.

Chauvaud L., Patry Y., Jolivet A., Cam E., Le Goff C., Strand Ø., Charrier G., Thébault J., Lazure P., Gotthard K., Clavier J., 2012. Variation in size and growth of the great scallop *Pecten maximus* along a latitudinal gradient. PLoS ONE 7(5): e37717. doi:10.1371/journal.pone.0037717

Christophersen G., Strand O., 2003. Effect of reduced salinity on the great scallop (*Pecten maximus*) spat at two rearing temperatures. Aquaculture, 215, 79–92.

1. Cowen R.K., Lwiza K.M.M., Sponaugle S., Limouzy-Paris C.B., Olson D.B., 2000. Connectivity of marine populations: open or closed? Science 287, 857–859.

Coum A., 1979. La population de crépidules *Crepidula fornicata* (L.) en rade de Brest: écologie et dynamique. PhD thesis, University of Western Brittany, Brest (France), 134 p.

Crochelet E., Roberts J., Lagabrielle E., Obura D., Petit M., Chabanet P., 2016. A model-based assessment of reef larvae dispersal in the Western Indian Ocean reveals regional connectivity patterns—potential implications for conservation policies. Reg. Stud. Mar. Sci. 7, 159–167.

Crowley P. H., Davis H. M., Ensminger A. L., Fuselier L. C., Kasi Jackson J., Nicholas McLetchie D., 2005. A general model of local competition for space. Ecology Letters, 8, 176–188.

Drake, P. T., Edwards, C. A., Morgan, S. G., Dever, E. P., 2013. Influence of larval behavior on transport and population connectivity in a realistic simulation of the California current system. J. Mar. Res. 71, 317–350.

Faure L., 1956. La coquille Saint-Jacques (*Pecten maximus* L.) en rade de Brest en 1952. CIEM, Ann. Biol. 9, 91–92

Fuchs H. L., Solow A. R., Mullineaux L. S., 2010. Larval responses to turbulence and temperature in a tidal inlet: habitat selection by dispersing gastropods? J. Mar. Res. 68, 153-188.

Guérin L., 2004. La crépidule en rade de Brest: un modèle biologique d'espèce introduite proliférante en réponse aux fluctuations de l'environnement. PhD thesis, University of Western Brittany, Brest (France), 426 p.

Hamon D., Blanchard M., 1994. Etat de la prolifération de la crépidule (*Crepidula fornicata*) en baie de St Brieuc. Rapport Ifremer DEL 94.14, 29 p.+annexes.

Holme, N. A., 1961. The bottom fauna of the English Channel. J. mar. biol. Ass. U.K., 41, 397-461.

Lazure P., Dumas F., 2008. An external–internal mode coupling for a 3D hydrodynamical model for applications at regional scale (MARS). Advances in Water Resources, 31(2), 233-250.

Leblanc N., Harmel B., Foucher E. 2011. Evaluation de l'impact des dragues à coquilles Saint-Jacques sur les communautés benthiques en baie de Seine. Rapport Ifremer/Comité Régional des Pêches Maritimes de Basse-Normandie, 39 p. + annexes, http://doi.org/10.13155/26747

Le Goff C., Lavaud R., Cugier P., Jean F., Flye-Sainte-Marie J., Foucher E., Desroy N., Fifas S., Foveau A., 2017. A coupled biophysical model for the distribution of the great scallop *Pecten maximus* in the English Channel. Journal of Marine Systems, 167, 55–67.

Levins R., 1969. Some demographic and genetic consequences of environmental heterogeneity for biological control. Bulletin of the Entomological Society of America, 15, 237-240.

Mayorga-Adame C. G, Batchelder H P., Spitz Y. H., 2017. Modeling Larval Connectivity of Coral Reef Organisms in the Kenya-Tanzania Region. Frontiers in Marine Science, 4, 92.

Ménesguen A., Dussauze M., 2015. Détermination des "bassins récepteurs" marins des principaux fleuves français de la façade Manche-Atlantique, et de leurs rôles respectifs dans l'eutrophisation phyto-planctonique des masses d'eau DCE et des sous-régions DCSMM. Rapport IFREMER/ONEMA, Thème 2 " Evolution, fonctionnement et évaluation des écosystèmes littoraux", Action N°14, 195 p. + annexes. http://archimer.ifremer.fr/doc/00333/44422/

Ménesguen A., Grégoris T., 2017. Modelling benthic invasion by the colonial gastropod *Crepidula fornicata* and its competition with the bivalve *Pecten maximus.* 1. A new 0D model for population dynamics of colony-forming species. . Ecol. Mod. 368, 277–287.

Nelson, W. G., 1978. The effects of mercury, silver and copper on the survival and growth of *Crepidula fornicata* larvae. M.S. thesis, University of Bridgeport, Bridgeport, Connecticut.

Nelson, D. A., Calabrese A., Greig R. A., Yevich P. P., Chang S., 1983. Long term silver effects on the marine gastropod *Crepidula fornicata*. Mar. Ecol. Prog. Ser. 12: 155–165.

Nicolle A., Dumas F., Foveau A., Foucher E., Thiébaut E., 2013. Modelling larval dispersal of the king scallop (*Pecten maximus*) in the English Channel: examples from the bay of Saint-Brieuc and the bay of Seine. Ocean Dynamics, 63(6), 661-678.

Nilsson Jacobi M., Jonsson P.R., 2011. Optimal networks of nature reserves can be found through eigenvalue perturbation theory of the connectivity matrix. Ecological Applications, 21, 1861-1870.

Paris, C. B., Chérubin, L., Cowen, R. K., 2007. Surfing, spinning, or diving from reef to reef: effects on population connectivity. Mar. Ecol. Prog. Ser., 347, 285–300.

Quiniou F., Blanchard M., 1987. Etat de la prolifération de la crépidule (*Crepidula fornicata* L.) dans le secteur de Granville (Golfe Normand-Beton - 1985). Haliotis, 16, 513-526.

Roughgarden J., Iwasa Y., Baxter C., 1985. Demographic theory for an open marine population with space-limited recruitment. Ecology 66, 54–67.

Sauriau, P.G., Pichocki-Seyfried, C., Walker, P., De Montaudouin, X., Palud, C., Héral, M., 1998. *Crepidula fornicata* L. (mollusque, gastéropode) en baie de Marennes-Oléron: cartographie des fonds par sonar à balayage latéral et estimation du stock. Oceanol. Acta 21, 353 – 362.

Savina M., Ménesguen A., 2008. A deterministic population dynamics model to study the distribution of a benthic bivalve with planktonic larvae (*Paphia rhomboides*) in the English Channel (NW Europe) .Journal of Marine Systems , 70(1-2), 63-76.

Sebens, K. P. 1982. Competition for space: growth rate, reproductive output, and escape in size. American Naturalist, 120, 189-197.

Thieltges D. W., Strasser M., van Beusekom J. E. E., Reise K., 2004. Too cold to prosper - winter mortality prevents population increase of the introduced American slipper limpet *Crepidula fornicata* in northern Europe. Journal of Experimental Marine Biology and Ecology 311, 375-391.

Thouzeau G., Chauvaud L., Grall J., Guérin L., 2000. Rôle des interactions biotiques sur le devenir du pré-recrutement et la croissance de *Pecten maximus* (L.) en rade de Brest. C R Acad. Sci. Paris, Sci. Vie, 323:815–825.

Tilman D., 1994. Competition and biodiversity in spatially structured habitats. Ecology, 75, 2–16.

Treml E.A., Halpin P.N., Urban D.L., Pratson L., 2008. Modeling population connectivity by ocean currents, a graph-theoretic approach for marine conservation. Landscape Ecology, 23, 19-36.

Wolanski E., 1994. Physical Oceanographic Processes of the Great Barrier Reef. CRC Press, Boca Raton, Florida. p. 194

**Table captions**

Table 1. Parameters used in the 2D model of slipper limpet and scallop populations.

| Parameter | Description | Unit | Value for slipper limpet | Value for scallop |
|---|---|---|---|---|
| m | Natural mortality rate | $y^{-1}$ | 0.1 | 0.15 |
| a | Probability of rearrangement of broken chains | $y^{-1}$ | 0.3 | - |
| b | Probability of anthropogenic chain break | $y^{-1}$ | 0.0 | - |
| α | Relative affinity for bare grounds | unitless | 0.01 | 1.0 |
| β | Relative affinity for slipper limpet beds | unitless | 1.0 | 0.6 |
| s | Survival probability of a pelagic larva | $y^{-1}$ | Regional: 0.015, Local: 0.1 | 0.000001 |
| $f_1, f_2$<br><br>$g_1, g_2$ | Parameters of the dose-response curve for :<br><br>-the effect of salinity on *Pecten* larvae<br><br>-the effect of heavy metal on *Crepidula* larvae | unitless | $1.45.10^{12}$, 1.0 | 181.3, 100 |

**Figure captions**

Figure 1. Observed general distribution of the slipper limpet on the NW European coasts (from Blanchard, 1997)

Figure 2. Recorded presence of slipper limpets in the French part (from Blanchard, 2012, top panel) and the English part (from the National Biodiversity Network's Gateway, bottom panel) of the English Channel.

Figure 3. Distribution of the slipper limpet observed in the bay of Brest (top panel: 1978, from Coum, 1979; bottom panel: 2013, from Carlier's pers. comm.)

Figure 4. Observed field distribution of the scallop at the local scale (top panel, from Thouzeau et al., 2000) and at the regional scale (bottom panel, from Le Goff et al., 2017).

Figure 5. Bathymetric grids used for the regional scale (left panel) and the local scale model (right panel).

Figure 6. Salinity stress on scallop larval survival: graph of the dose-response relationship (left), fitness map at local scale (middle) and regional scale (right).

Figure 7. Toxic stress on slipper limpet larval survival: graph of the dose-response relationship (left), fitness map at local scale (middle) and silver concentrations in oyster flesh measured at two ROCCH monitoring stations (right).

Figure 8. First eigenvalues of the connectivity matrix ranked by decreasing order of their modules at the regional scale (top panel) and at local scale (bottom panel).

Figure 9. Main eigenmodes of the connectivity matrix, at the regional scale (top panel) and at local scale (bottom panel). Colours refer to the local module of the eigenvector.

Figure 10. Three phases of slipper limpet colonization of the bay of Brest/bay of Douarnenez domain when inoculation has been done only in one mesh in the bay of Brest and in one mesh in the bay of Douarnenez. Colours refer to the animal abundance (ind.m$^{-2}$).

Figure 11. Simulated steady state mean distribution of the slipper limpet alone without (top panel) or with silver toxicity in the Aulne plume (bottom panel).

Figure 12. Successive phases of colonization of the bay of Biscay-English Channel domain, in terms of bottom coverage (%). Cases of slipper limpet inoculation done only in the bay of Seine (upper panel), scallop inoculation done in the Atlantic bay of Marennes-Oléron (middle panel) or scallop inoculation near the

Isles of Scilly (lower panel). Colours refer to the animal abundance (ind.m$^{-2}$). The black star in the first image of each row points to the inoculum mesh.

Figure 13. Simulated steady state distribution of the slipper limpet at the regional scale: mean abundance (left panel) and mean chain length (right panel).

Figure 14. Simulated steady state vs. observed distributions of the length of slipper limpets chains in the Golfe Normand-Breton (western English Channel).

Figure 15. Waves in the scallop bottom coverage: two opposite phases of the stationary wave in the bay of Brest (top panel) and two successive phases of the progressive wave at the regional scale (bottom panel). Colours refer to the bottom coverage by the individual "vital" areas (%).

Figure 16. Steady state distribution of scallop at the local scale: mean abundance, half-amplitude and period of possible limit cycle, without ($\beta = 1.0$, upper panel) or with a moderate ($\beta = 0.5$, lower panel) competition with the slipper limpet.

Figure 17. Steady state distribution of scallop at the regional scale: mean abundance, half-amplitude and period of possible limit cycle, without ($\beta = 1.0$, upper panel) or with a moderate ($\beta = 0.5$, lower panel) competition with the slipper limpet.

**Figures**
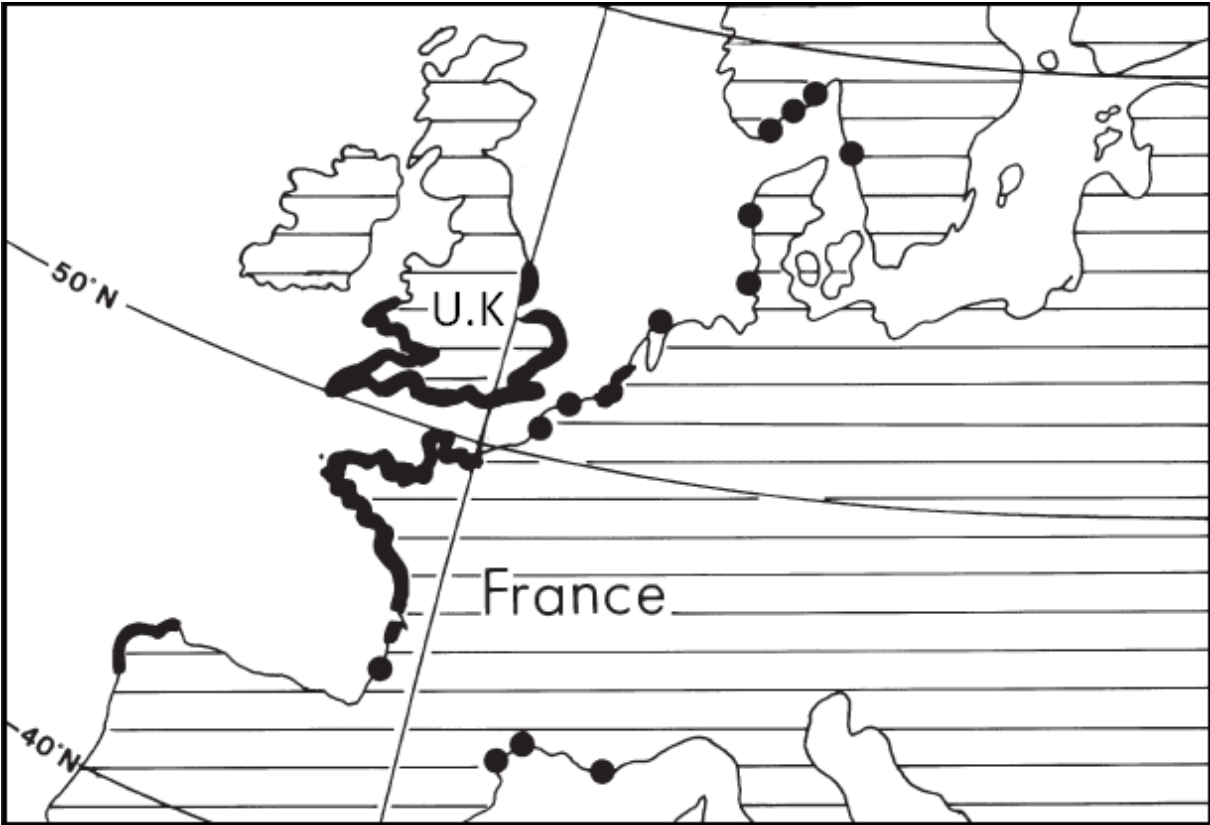


Figure 1
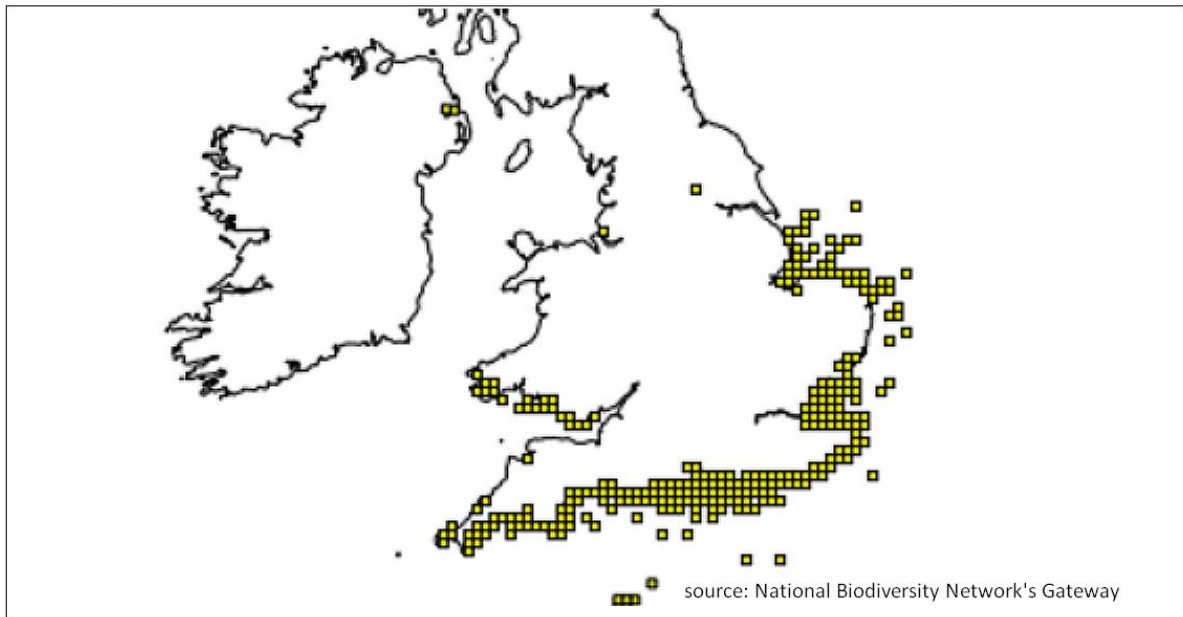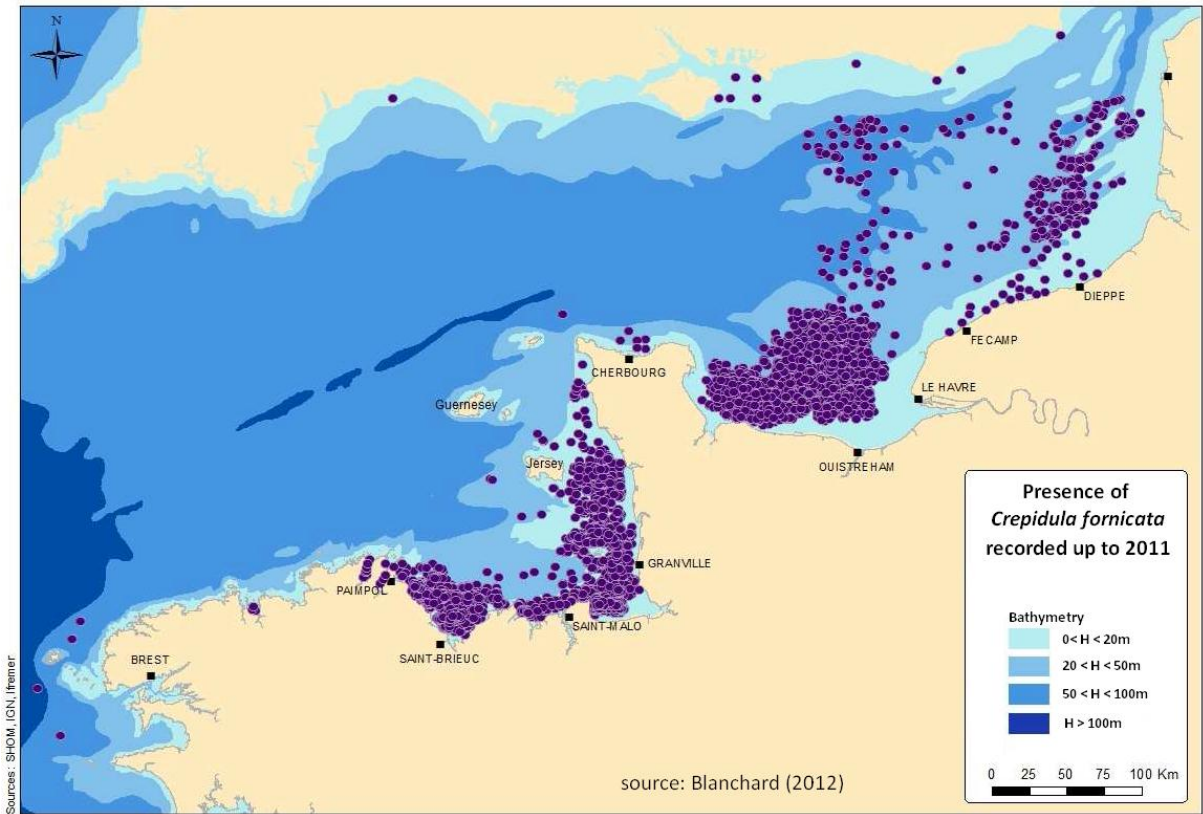
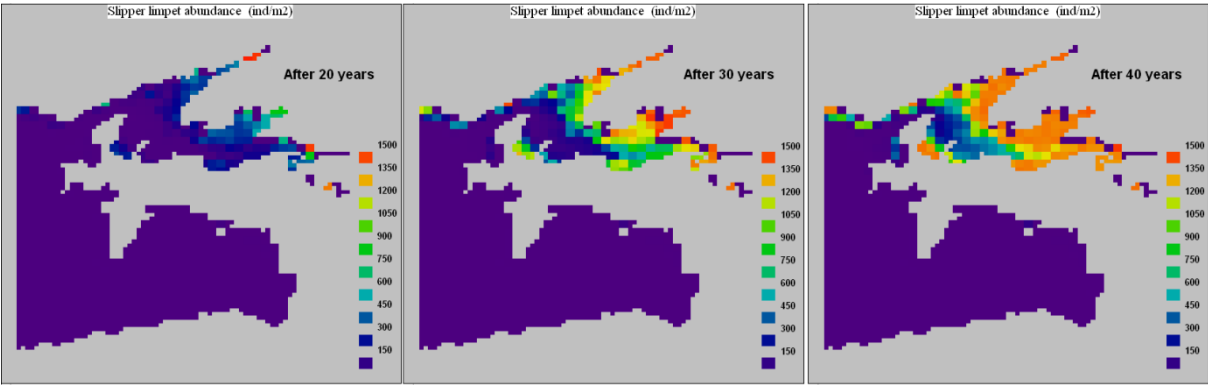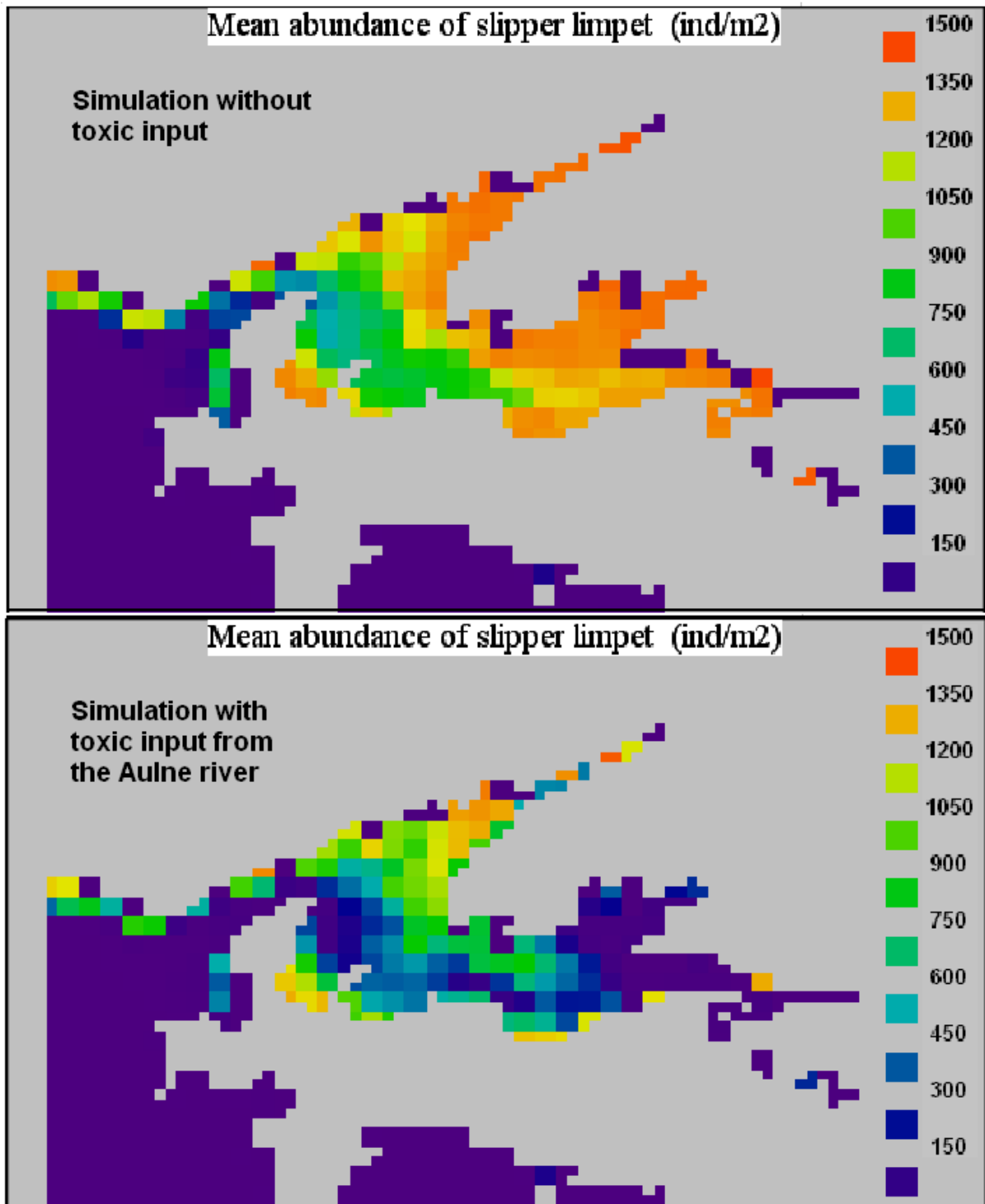Figure 2
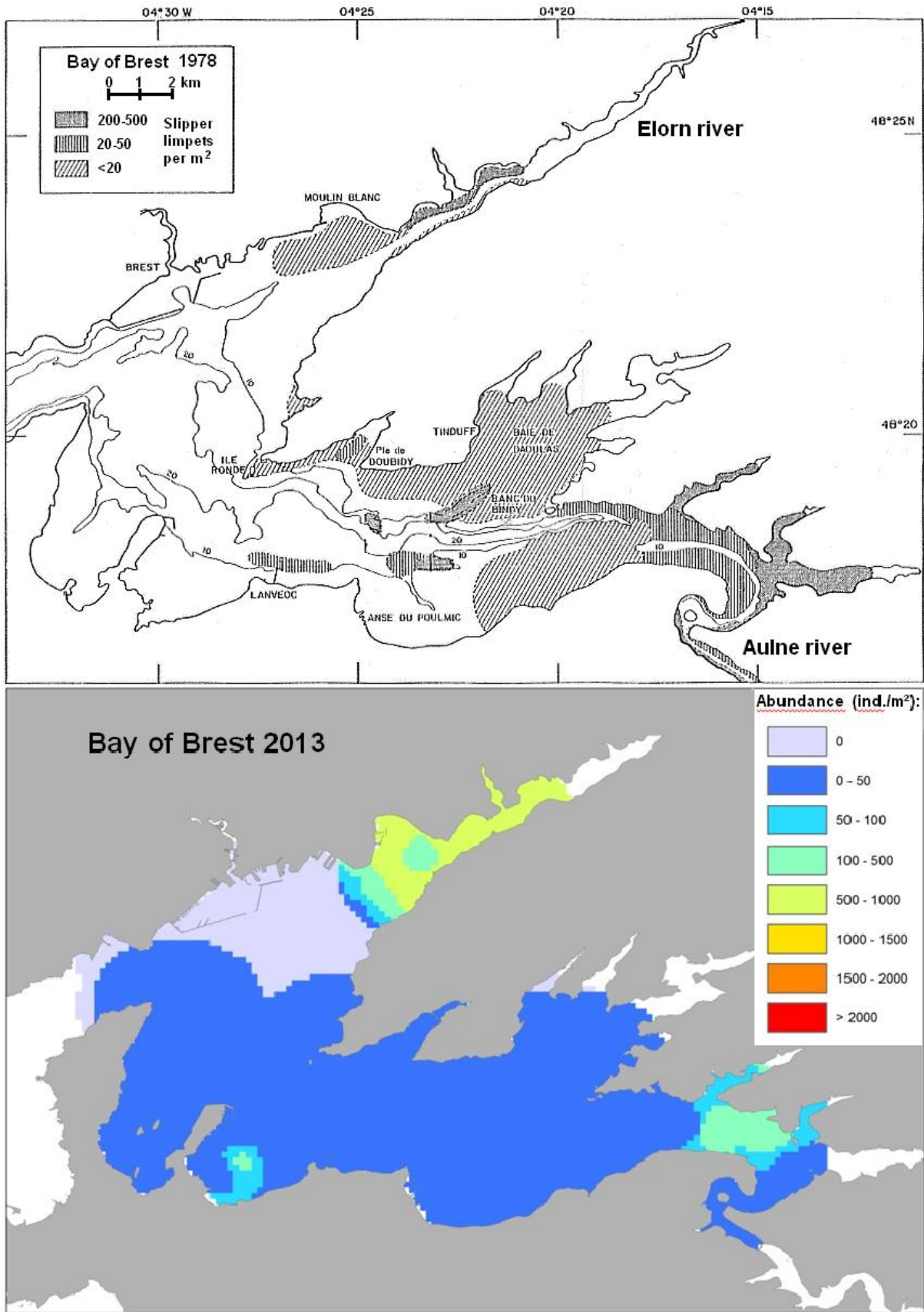
Figure 3
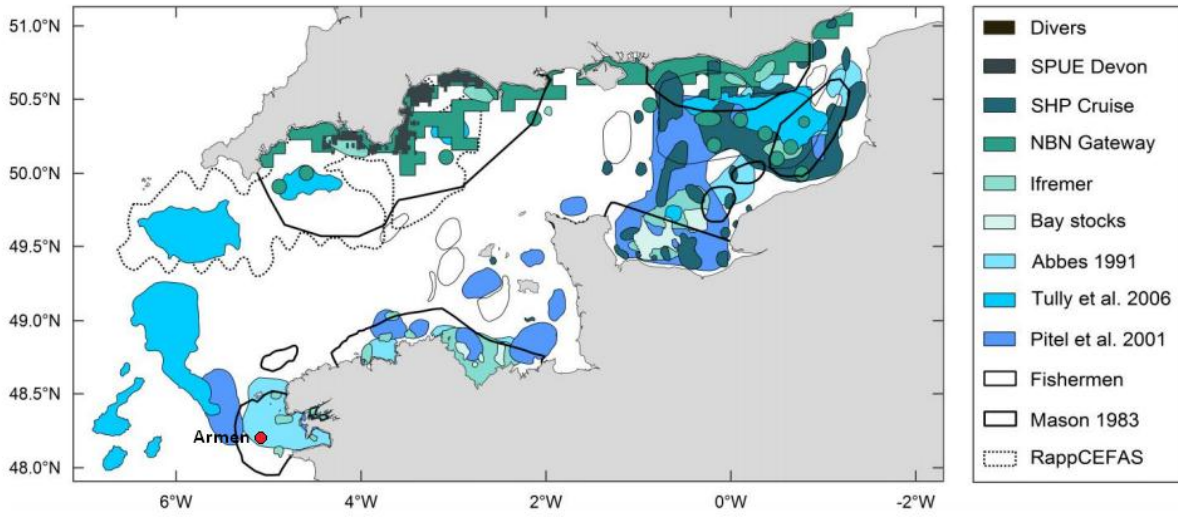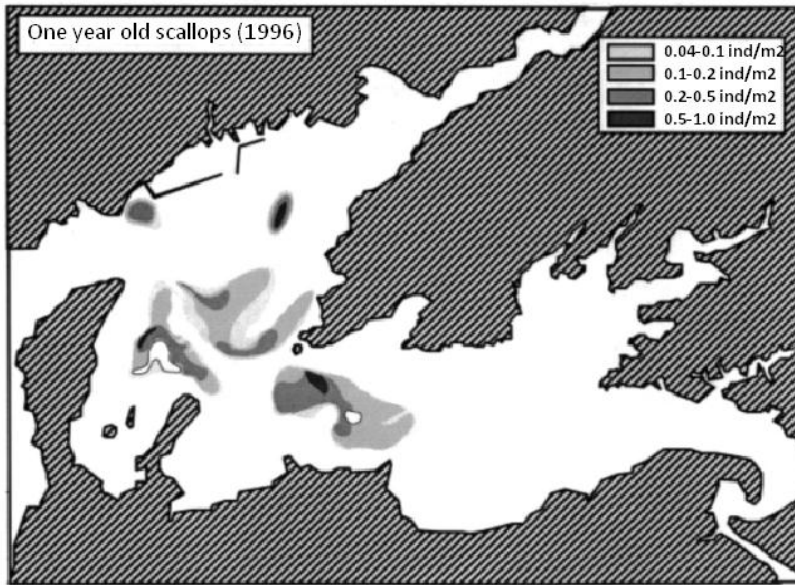
Figure 4
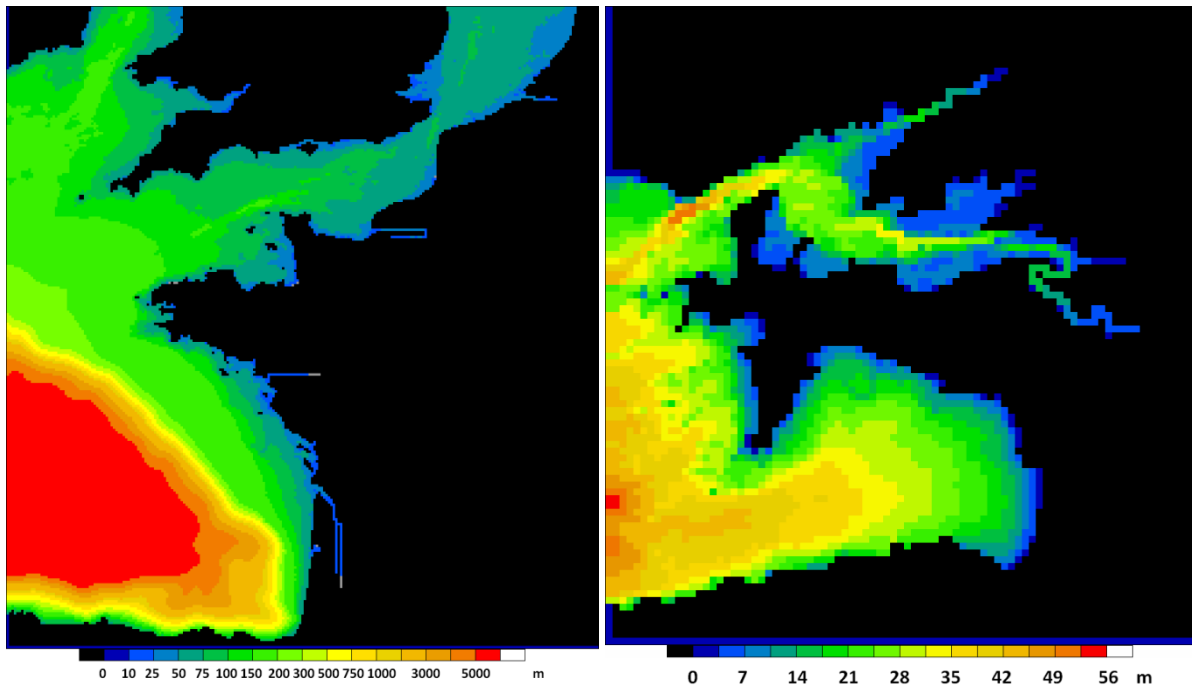
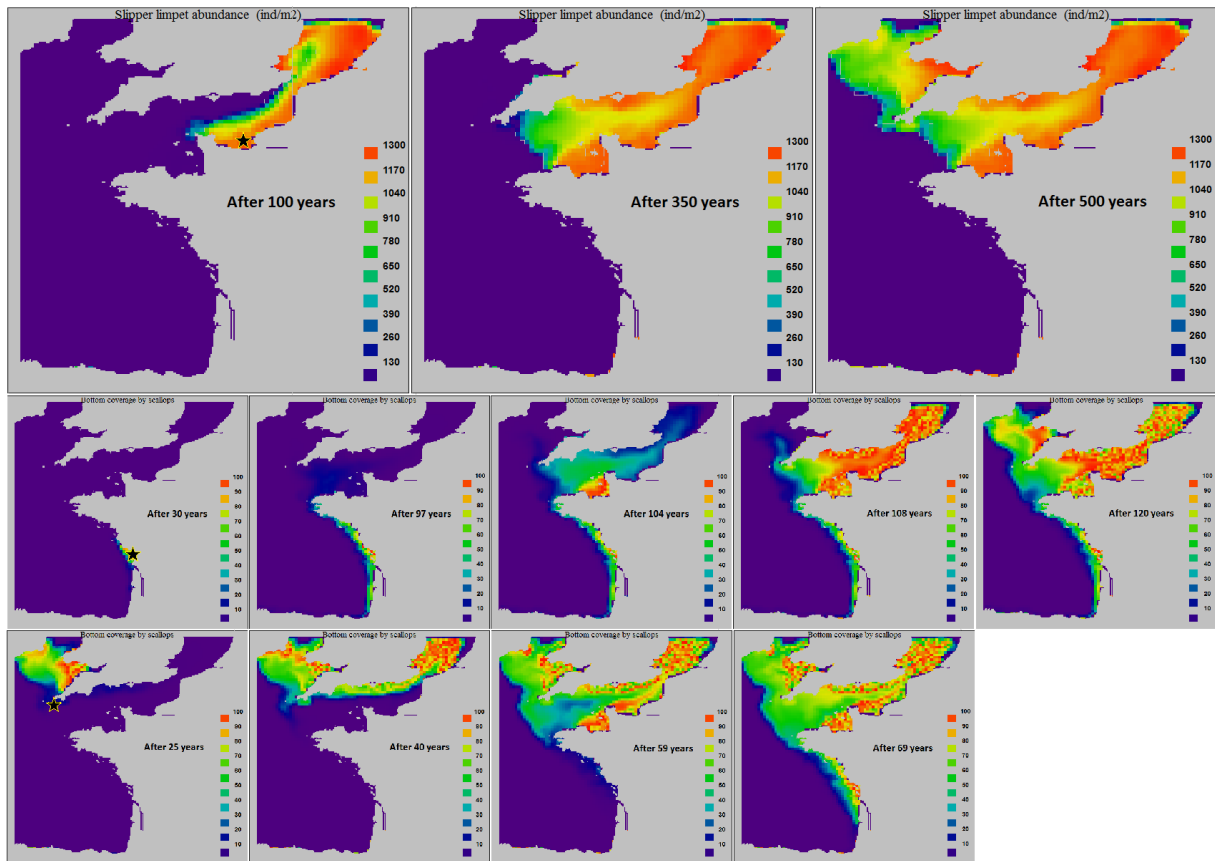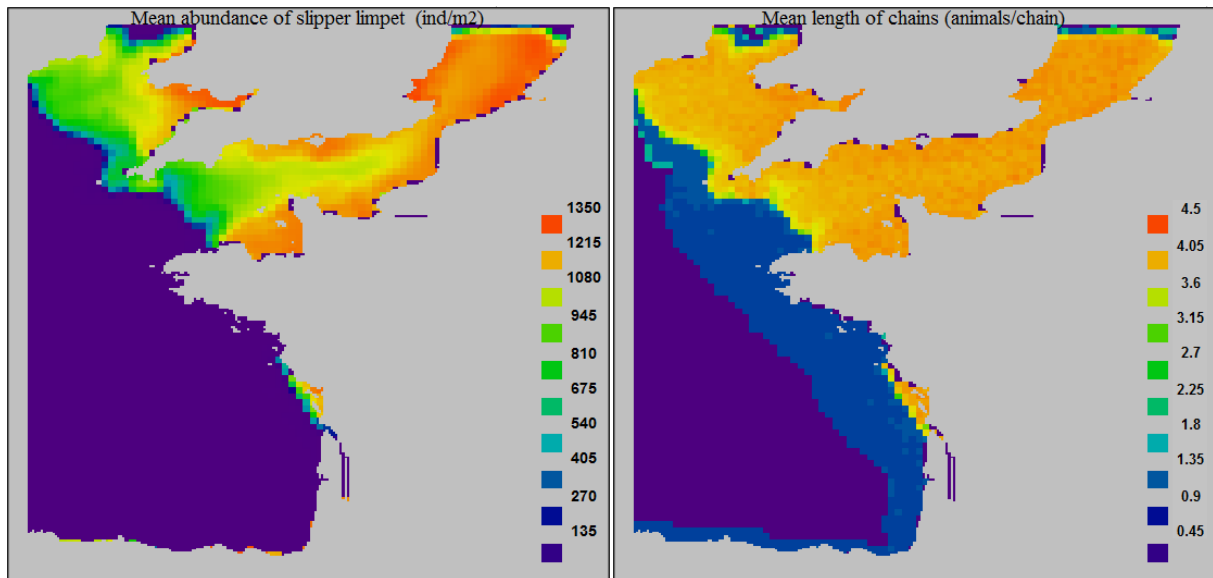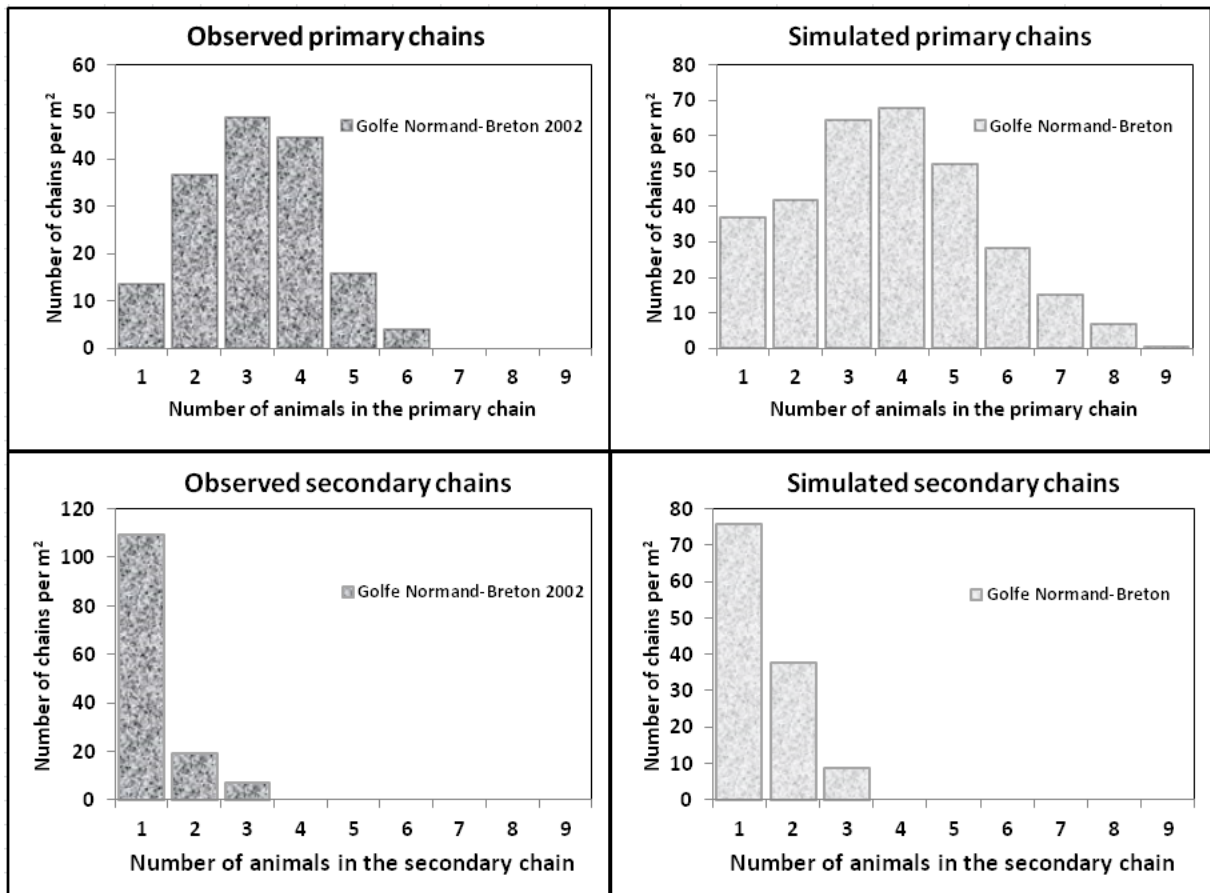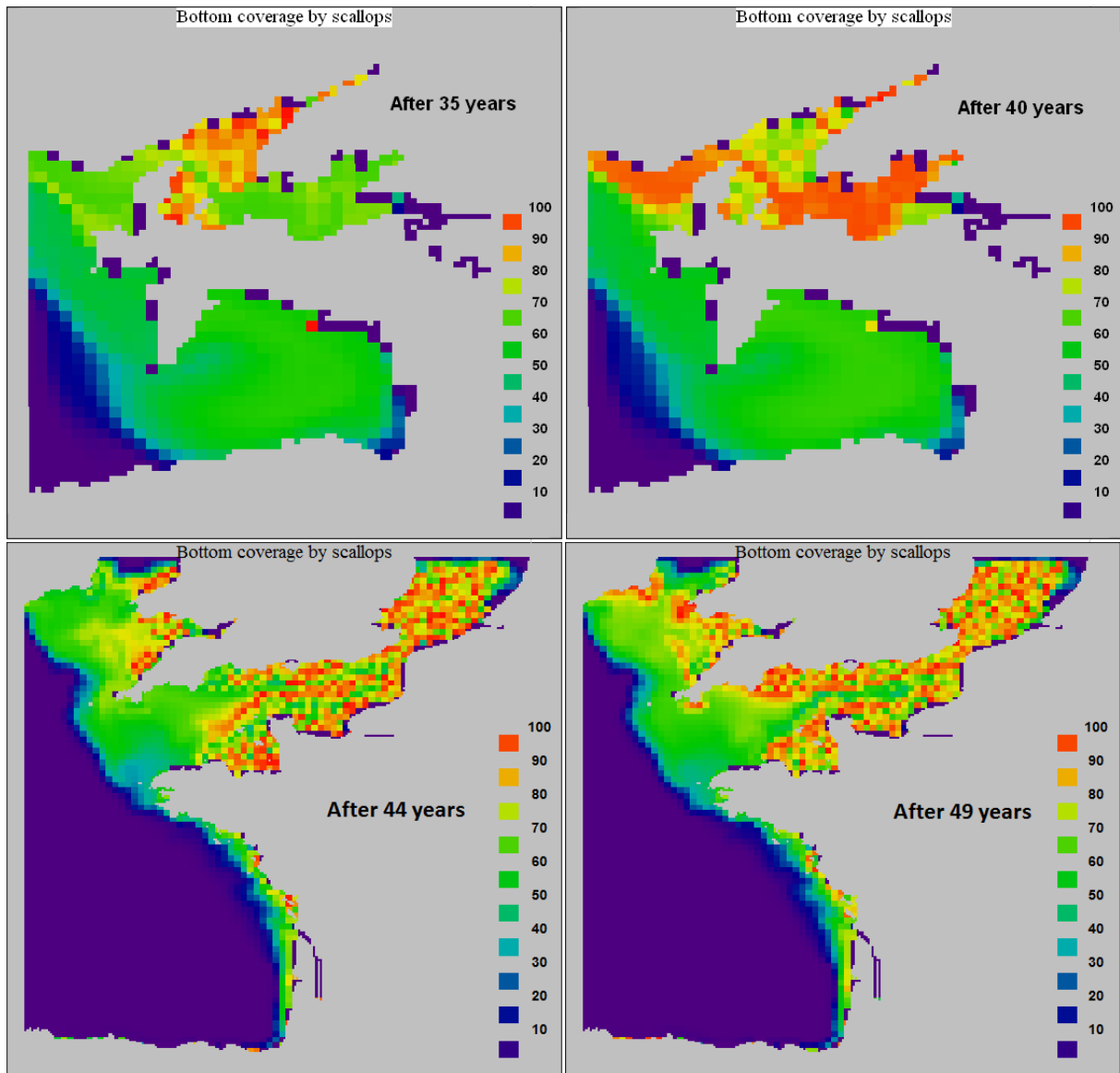Figure 5
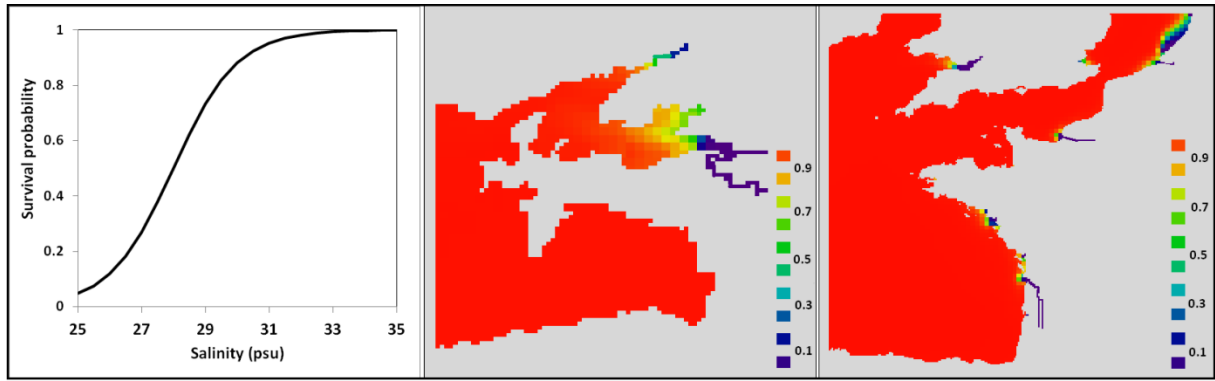
Figure 6
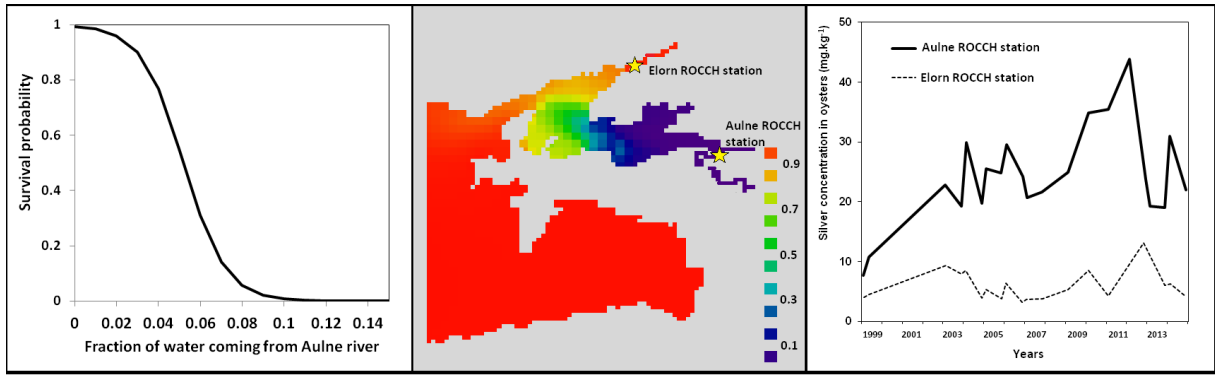
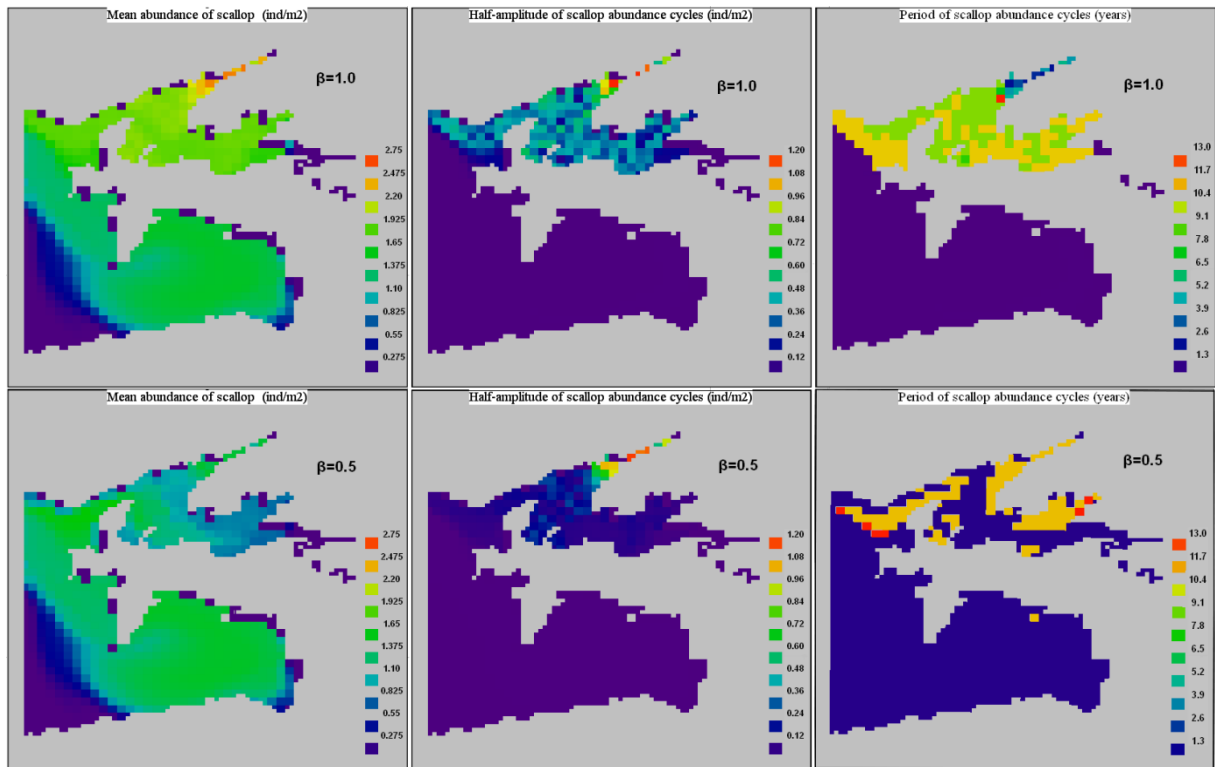Figure 7
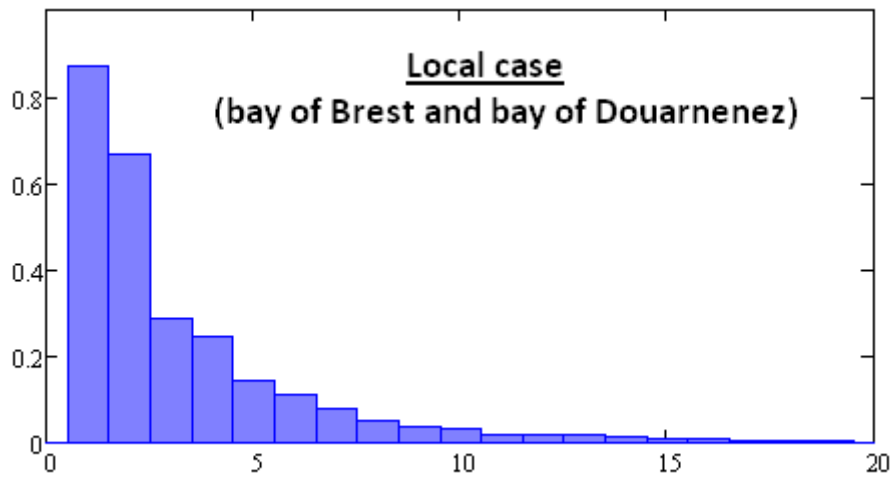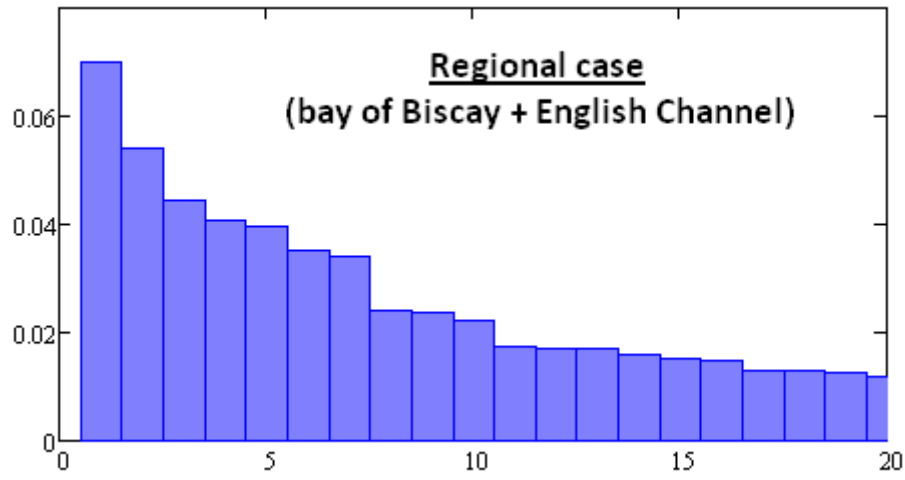
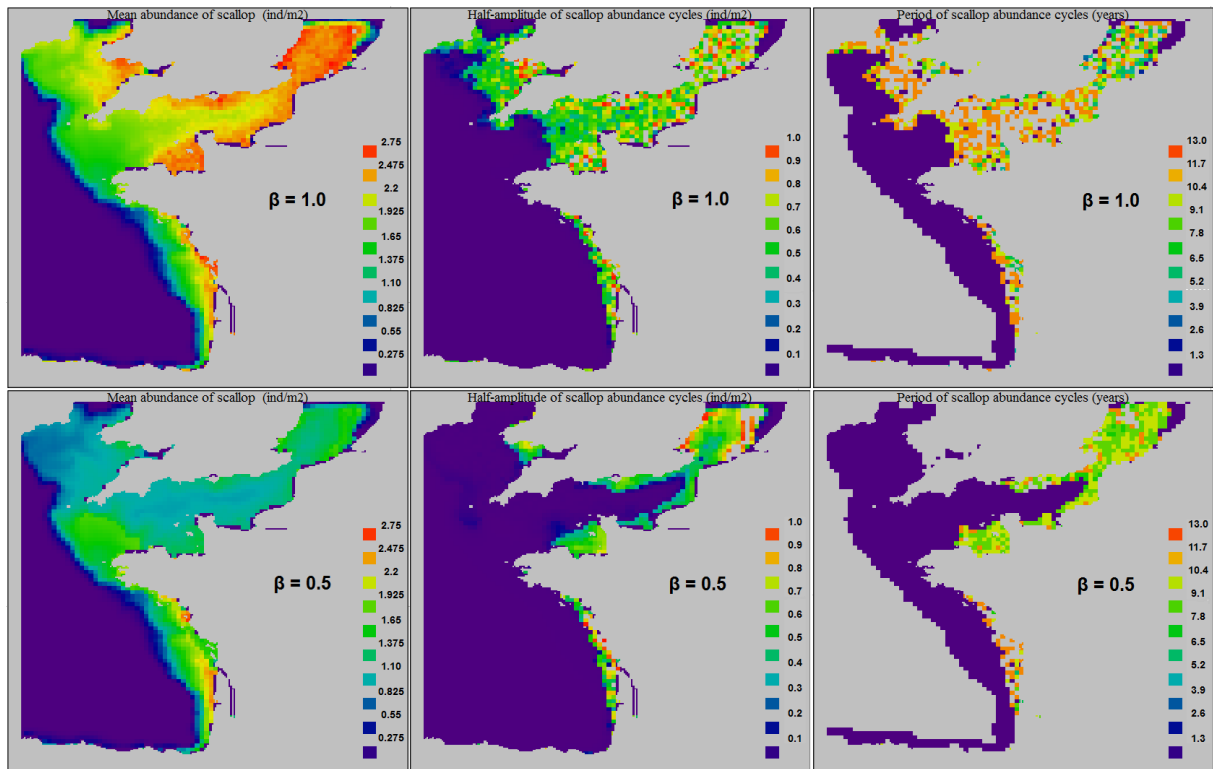Figure 8
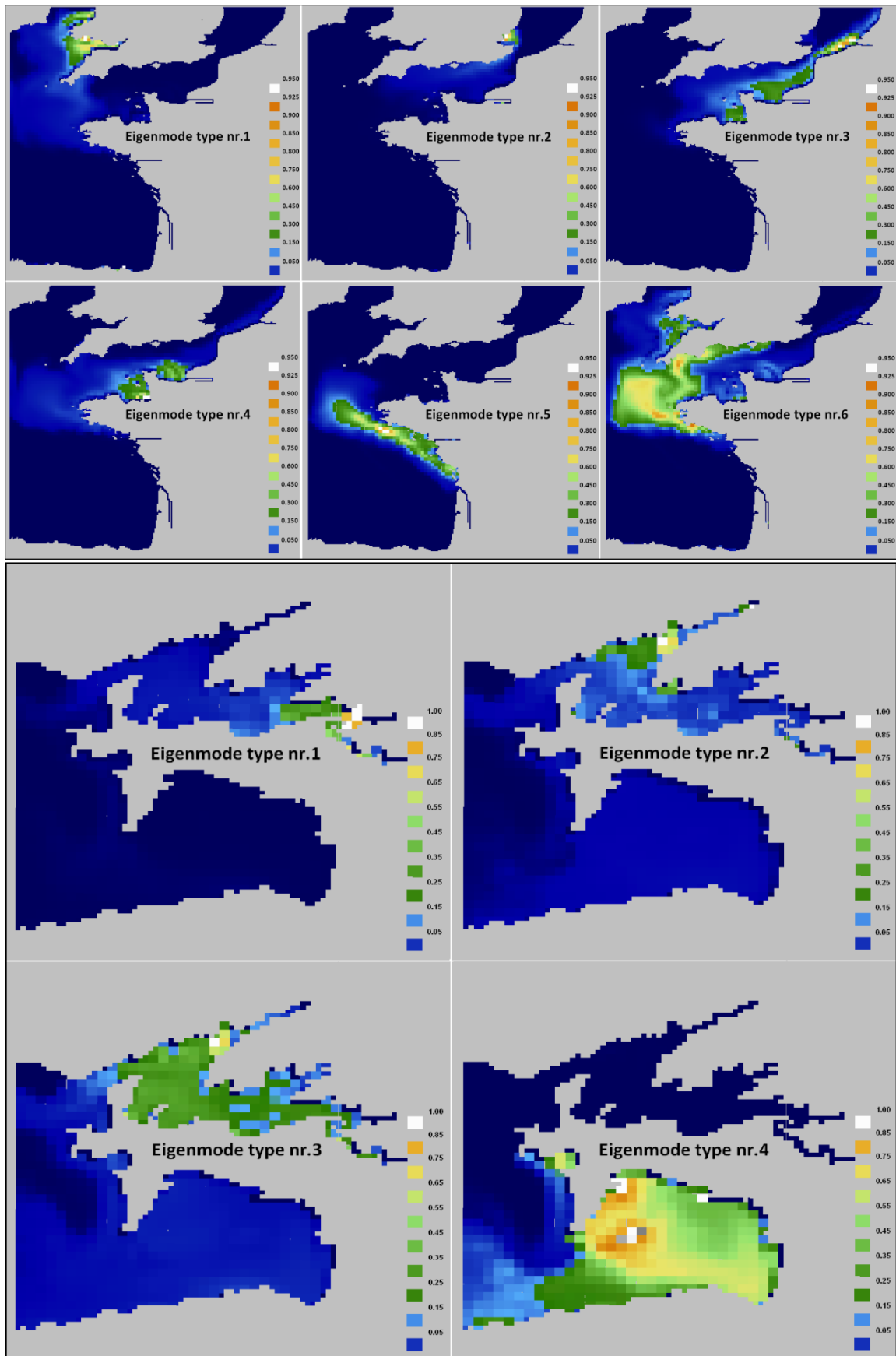
Figure 9

Figure 10

Figure 11

Figure 12

Figure 13

Figure 14

Figure 15

Figure 16

Figure 17